Molecular Therapy
Oncolytics
Original Article

AMERICAN SOCIETY of GENE & CELL THERAPY

Endogenous Akt Activity Promotes Virus Entry and Predicts Efficacy of Novel Chimeric Orthopoxvirus in Triple-Negative Breast Cancer

Audrey H. Choi,[1] Michael P. O'Leary,[1] Jianming Lu,[1] Sang-In Kim,[1] Yuman Fong,[1,2] and Nanhai G. Chen[1,2,3]

[1]Department of Surgery, City of Hope National Medical Center, Duarte, CA, USA; [2]Center for Gene Therapy, Department of Hematology and Hematopoietic Cell Transplantation, Beckman Research Institute, City of Hope National Medical Center, Duarte, CA, USA; [3]Gene Editing and Viral Vector Core, Beckman Research Institute, City of Hope National Medical Center, Duarte, CA, USA

Triple-negative breast cancer (TNBC) is an aggressive subtype of breast cancer with high recurrence rate and poor prognosis. Here, we describe a novel, chimeric orthopoxvirus (CF33) that efficiently kills TNBC. Cytotoxicity was assayed *in vitro* in four TNBC cell lines. Viral replication was examined through standard plaque assay. Two orthotopic TNBC xenograft models were generated in athymic nude mice and were injected with CF33 intratumorally. CF33 was effective *in vitro* with potent cytotoxicity and efficient intracellular replication observed in TNBC lines with phosphatidylinositol 3-kinase (PI3K)/Akt pathway mutations that resulted in endogenous phospho-Akt (p-Akt) activity (BT549, Hs578T, and MDA-MB-468). Relative resistance to CF33 by wild-type PI3K/Akt pathway cell line MDA-MB-231 was overcome using higher MOI. The virus was effective *in vivo* with significant tumor size reduction in both xenograft models. Mechanistically, CF33 appears to share similar properties to vaccinia virus with respect to Akt-mediated and low-pH-mediated viral entry. In summary, CF33 demonstrated potent antitumoral effect *in vitro* and *in vivo*, with the most potent effect predicted by the presence of endogenous Akt activity in the TNBC cell line. Further investigation of its mechanism of action as well as genetic modifications to enhance its natural viral tropism are warranted for preclinical development.

INTRODUCTION

Triple-negative breast cancer (TNBC) continues to remain a treatment challenge in the field of oncology, given its poor prognosis and higher recurrence rates compared to receptor-positive disease.[1] Because TNBC by definition lacks estrogen receptor (ER), progesterone receptor (PR), and human epidermal growth factor receptor 2 (HER2) expression, the mainstay of adjuvant therapy is systemic cytotoxic chemotherapy.[2]

Although efforts to define new molecular targets for TNBC treatment continue, recent US Food and Drug Administration (FDA) approval of the first oncolytic virus for use in man has led to renewed interest in developing viral therapies for many types of cancer.[3] Oncolytic viruses exploit a number of methods to naturally target and infect tumor cells, including cell surface receptor mimicry or utilization of aberrantly upregulated signaling pathways to infect the target cell. Once viral infection occurs, the target cell is destroyed by either direct oncolysis or by the host's own immune system directed against the tumor cells by the inciting viral infection.[4]

Here, we present data on a novel chimeric orthopoxvirus developed in our laboratory that demonstrates effective antitumor properties both *in vitro* and *in vivo* in TNBC models. We also investigate the mechanism of action of this novel virus and how its efficacy may be related to intrinsic properties of the TNBC cell lines themselves.

RESULTS

Chimeric Orthopoxvirus CF33 Effectively Kills TNBC *In Vitro*

CF33 demonstrates both time- and dose-dependent cytotoxicity against four different TNBC cell lines. In the BT549, Hs578T, and MDA-MB-468 cell lines, CF33 killed over 80% of cancer cells at day 6 of treatment with an MOI of 1 (Figures 1A–1C). The last cell line MDA-MB-231 demonstrated relative resistance, requiring an MOI of 10 to achieve comparable effect (Figure 1D).

CF33 Replication in TNBC Lines Correlates with Cytotoxicity

Viral replication was studied by observing CF33 replication (MOI 0.01) in all four cell lines over 72 hr. Viral replication was efficient in BT549, Hs578T, and MDA-MB-468, with peak replication occurring in the 48- to 72-hr range (Figure 2). CF33 did not replicate well in MDA-MB-231, suggesting that its relatively poor cytotoxicity may be related to ineffective replication within or inefficient entry into the cell.

Received 6 March 2018; accepted 1 April 2018;
https://doi.org/10.1016/j.omto.2018.04.001.

Correspondence: Nanhai G. Chen, PhD, Department of Surgery, City of Hope National Medical Center, 1500 E. Duarte Road, Rm 1102, Familian Science Building, Duarte, CA 91010, USA.
E-mail: nchen@coh.org

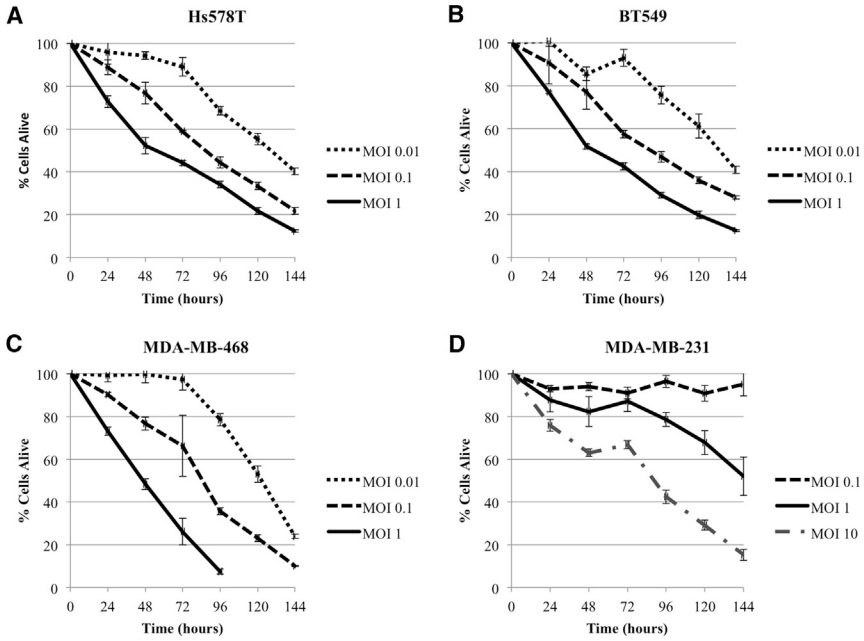

Figure 1. Time- and Dose-Dependent Cytotoxicity of CF33 in Four Triple-Negative Breast Cancer Lines

(A–D) Hs578T (A; LD50 MOI 0.058; SD 0.032), BT549 (B; LD50 MOI 0.069; SD 0.033), and MDA-MB-468 (C; LD50 MOI 0.129; SD 0.073) all demonstrate effective cytotoxicity at low MOI, whereas MDA-MB-231 (D; LD50 MOI 5.585; SD 1.747) required one log higher MOI to achieve similar effect. LD50 (at 96 hr), median lethal dose.

Endogenous Phospho-Akt Activity in TNBC Corresponds to CF33 Cytotoxicity and Growth Curve Patterns

Untreated TNBC cell lysates were evaluated for endogenous phospho-Akt (p-Akt) activity, given that three of four cell lines harbor known mutations in the Akt/phosphatase and tensin homolog (PTEN) pathway. Analysis by western blot showed a low basal level of endogenous p-Akt activity in Hs578T, BT549, and MDA-MB-468, which all have mutations in PIK3R1 and PTEN genes, respectively (Figure 3A, left). MDA-MB-231 did not demonstrate baseline p-Akt activity and does not have a known mutation in the Akt/PTEN signaling pathway. Treatment with CF33 only slightly increased p-Akt activity in MDA-MB-231 after 24 hr (Figure 3A, right). In fact, closer examination of the signaling patterns over 24 hr revealed CF33 treatment induced preferential cell signaling via p-extracellular-signal-regulated kinase (ERK) rather than p-Akt in MDA-MB-231. By contrast, MDA-MB-468 demonstrated gradual increase in p-Akt signal strength over 24-hr viral treatment with abolishment of its endogenous p-ERK signaling (Figure 3B).

CF33 Entry Is More Efficient in TNBC Lines with Endogenous Akt Activity

In order to assess viral entry in the different TNBCs, CF33 was modified to express the luciferase gene (33-(SE)Fluc2) under control of the vaccinia virus synthetic early promoter (SE) such that luciferase activity following viral infection could act as a surrogate to quantify the relative amounts of virus entering the cells. As vaccinia virus infection has been demonstrated in the literature to be enhanced by low pH, buffers with pH ranging from 3 to 7 were used following viral adsorption at 4°C. 33-(SE)Fluc2 entry was stimulated by pH in the 4 or 5 range for all four TNBC cell lines. However, at neutral pH 7, 33-(SE)Fluc2 entry was more efficient in TNBC cell lines with endogenous p-Akt activity (BT549, Hs578T, and MDA-MB-468) compared to the cell line without endogenous p-Akt activity (MDA-MB-231; Figure 4). Viral entry appears to correlate with the data on CF33 cytotoxicity and intracellular replication within these cell lines.

Akt Inhibitor LY294002 Most Effectively Blocks 33-(SE)Fluc2 Entry in the Akt-PTEN Wild-Type Cell Line MDA-MB-231

Because 33-(SE)Fluc2 entry appears to correlate with p-Akt status, viral entry was measured in the presence of the Akt pathway inhibitor LY294002 (blocks phosphatidylinositol 3-kinase [PI3K]) at 0, 25, and 50 μM. Compared to untreated controls, all cell lines demonstrated reduction in 33-(SE)Fluc2 entry with LY294002. At 50 μM, MDA-MB-231 (wild-type for Akt/PTEN pathway mutation) demonstrated the largest reduction (86%) in 33-(SE)Fluc2 entry compared to untreated control. Other cell lines with Akt/PTEN pathway mutations exhibited decreased sensitivity to viral entry inhibition by LY294002 treatment (Figure 5).

Intratumoral Injection of CF33 Effectively Reduces Tumor Size in the MDA-MB-468 Xenografts while Inhibiting Tumor Growth in the MDA-MB-231 Xenografts

In order to determine the effect of CF33 *in vivo*, two xenograft models were created by implanting MDA-MB-468 and MDA-MB-231 cells into the mammary fat pads of athymic nude mice. Tumors in the MDA-MB-468 group were treated with either PBS or CF33 (10^3 plaque forming units [PFU] or 10^4 PFU per tumor). Because MDA-MB-231 demonstrated the most resistance to CF33 treatment *in vitro*, these tumors were treated with either PBS or CF33 at 10^5 PFU per tumor. MDA-MB-468 xenografts exhibited significant reduction in tumor size at post-treatment day 15 in both treatment groups, and this effect was sustained 5 weeks after injection (Figure 6). There was no significant systemic toxicity as determined by body weight measurements following viral injection. MDA-MB-231 xenografts treated with CF33 demonstrated significant inhibition in tumor growth starting at post-injection day 7 compared to control (Figure 7). There was marked weight loss in one mouse that was shown to have intraperitoneal disease at time of necropsy, likely due to inadvertent intraperitoneal injection during tumor implantation. This mouse was excluded from the final analysis. There were no other mice with signs of systemic toxicity from the viral treatment, although one mouse was noted to have cutaneous pox lesion on its hind paw.

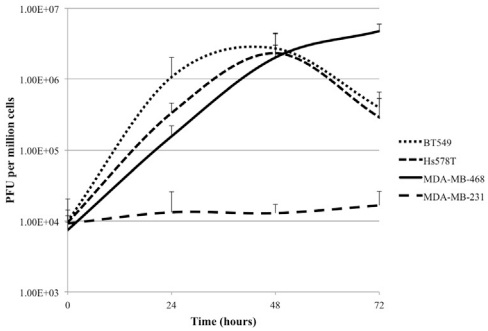

Figure 2. CF33 Replication in Triple-Negative Breast Cancer Cell Lines Correlates with *In Vitro* Cytotoxicity Results

CF33 replicates effectively in BT549, Hs578T, and MDA-MB-468 cell lines, whereas viral replication was relatively poor in MDA-MB-231. All growth curves performed at MOI 0.01. Data are presented as means ± SD of the means.

Viral Biodistribution of CF33 in the MDA-MB-468 Xenograft Model at One and Six Weeks Post-treatment Demonstrates Natural Viral Tropism for Tumor Tissue

One and six weeks following treatment of the tumors with 10^4 PFU of CF33, three mice from each group were sacrificed to determine the viral distribution in tumor and various organs. Viral titers of infected tumor tissue exhibit at least three log higher titer of CF33 compared to healthy organs (Figure 8), demonstrating the natural tropism of the unmodified virus for tumor cells. At six weeks post-injection, a reduction in viral titer is observed across all organs, which likely represents some degree of viral clearance from the body. However, viral titer in tumor tissue remains high in tumor tissue even at six weeks post-treatment.

Infection of CF33 in Orthotopic Xenograft Model Confirmed by Immunofluorescent Imaging

One week after CF33 injection, immunofluorescent detection of polyclonal antibody against vaccinia virus proteins demonstrates viral infection of MDA-MB-468 tumor tissue treated with CF33 compared to control (Figure S1).

DISCUSSION

Our data show that CF33 was effective *in vitro* against several different TNBC cell lines. Sensitivity to infection by CF33 with subsequent intracellular growth and cytotoxicity was predicted by the level of endogenous p-Akt activity secondary to presence of PI3K/Akt pathway mutation in the TNBC lines. CF33 was also effective *in vivo*, demonstrating significant reductions in tumor size in two different TNBC xenograft models when delivered via intratumoral injection.

Genetic sequencing demonstrates that CF33 is closely related to vaccinia virus (VACV), although full genomic comparison of CF33 to its parental viruses has not been performed due to lack of complete genetic sequences for several parental strains. Many of CF33's properties with respect to cellular entry mechanism are consistent with what we know about VACV and other orthopoxviruses. Two modes of cellular entry have been described for VACV, and cellular entry of VACV has been shown to vary depending on the viral strain and the target cell type.[7] The first mode is direct membrane fusion mediated by proteins on the viral envelope. These proteins interact with host cell receptors, leading to fusion of the viral envelope with the plasma membrane of the host cell and release of virus into the cytoplasm.[8] The second is a pH-dependent endosomal process. Townsley and colleagues have previously shown that VACV entry and productive infection of the target cell is accelerated by a brief exposure to low pH.[9] CF33 also demonstrated similar behavior, with viral entry occurring maximally at pH 4 or 5. They suggest that VACV's ability to enter the cell in different ways contributes to the virus' wide host range.

Akt, otherwise known as protein kinase B, is a serine/threonine kinase that plays a central role in the regulation of growth and survival processes in normal cells. When growth factors and cytokines bind to their respective receptor tyrosine kinases and G-protein-coupled receptors, PI3K is activated. PI3K converts phosphatidylinositol-4,5-bisphosphate (PIP2) into phosphatidylinositol-3,4,5-trisphosphate (PIP3), which serves as a docking station for lipid-binding domains, such as the pleckstrin homology of Akt. When this occurs, Akt is phosphorylated at the Thr308 and Ser473 positions, activating its downstream effectors that are central to promoting cellular proliferation and inhibiting apoptosis.[8,10]

Previous studies have documented a variety of viruses that capitalize on the PI3K/Akt pathway to enter target cells, including influenza virus, hepatitis C virus (HCV), herpes simplex virus-1 (HSV-1), and avian leucosis virus (ALK).[11–14] It is hypothesized that cellular entry via endocytosis is a common mechanism among many viruses because it helps evade host immune detection longer, promoting the viral life cycle.[8] In the case of VACV, viral infection has also been shown to activate the Akt pathway. Izmailyan and colleagues[15] report that integrin beta-1 co-localizes with VACV on the target cell membrane prior to viral entry and that this interaction activates PI3K/Akt signaling.

The endogenous p-Akt status may also be related to sensitivity to viral infection. Wang and colleagues have shown that permissiveness to infection with myxoma virus, which is a member of the poxvirus family, correlated with the presence of endogenous p-Akt activity in cancer cells, not necessarily with cancer origin or cell type.[16] CF33 demonstrated a similar pattern in the TNBC lines we tested. Viral entry was more efficient in cell lines with endogenous p-Akt activity (Hs578T, BT549, and MDA-MB-468) than in the cell line without baseline p- Akt activity (MDA-MB-231). High rates of viral entry correlated with increased intracellular replication and better cytotoxicity in our *in vitro* studies.

The presence of endogenous p-Akt signals in these cell lines corresponded with known mutations in the PI3K/Akt pathway. Mutations in this pathway are frequently encountered in human cancers, accounting for 3%–5% of mutations observed.[10,17,18] PI3K/Akt pathway mutations occur at a higher rate in breast cancer, with *PIK3CA*

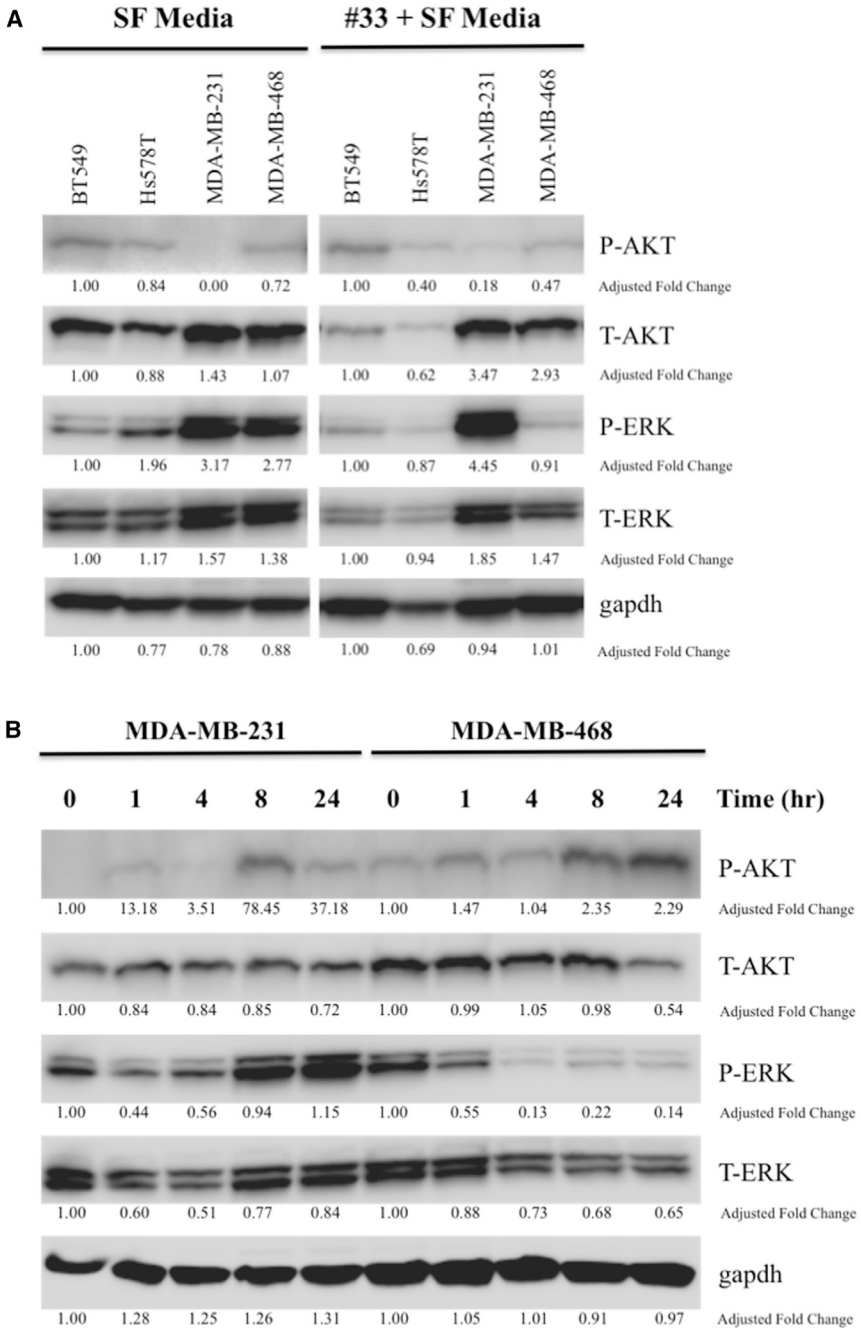

Figure 3. Western Blots of Triple-Negative Breast Cancer Cells before and after Treatment with CF33 Reveal Differences in Basal Endogenous p-Akt Activity as well as Inducible p-Akt Activity

(A) BT549, Hs578T, and MDA-MB-468 cell lines demonstrate low-level basal endogenous p-Akt activity in serum-free media (SF media), whereas MDA-MB-231 does not. Treatment with CF33 over 24 hr (right) appears to slightly induce p-Akt activity in MDA-MB-231. Endogenous p-Akt activity correlates with known mutations in the Akt/PTEN signaling pathways—BT549 (PTEN), Hs578T (PIK3R1), and MDA-MB-468 (PTEN). MDA-MB-231 does not have an Akt/PTEN mutation. Adjusted fold change is shown. (B) Examination of signaling patterns at different time points over 24 hr shows CF33 preferentially induces signaling in the p-ERK pathway in MDA-MB-231 line, whereas viral treatment induces p-Akt signaling in MDA-MB-468.

mutations most common (30%).[19] Similarly, TNBC also demonstrates higher rates of PI3K mutations than other human cancers but also carries more frequent PTEN mutations than receptor-positive breast cancer.[20] BT549 and MDA-MB-468 both have mutations in the *PTEN* gene.[21] Under normal cellular conditions, PI3K converts PIP2 to PIP3, which then goes on to phosphorylate Akt.[22] PTEN reverses the action of PI3K, converting PIP3 back to PIP2, such that mutations in *PTEN* result in constitutively active p-Akt. Hs578T has a mutation in *PIK3R1*,[23,24] the gene that encodes the regulatory p85α subunit of the PI3K heterodimer. When PI3K is activated, the inhibitory action of p85α is relieved, allowing the p110 catalytic subunit to activate PIP3.[25,26] Thus, mutations in *PIK3R1* result in loss of that inhibitory signal and constitutive activation of PIP3 and Akt. MDA-MB-231 has no known mutation in the PI3K/Akt pathway. If the PI3K/Akt pathway is activated during some viral infections and facilitates viral replication, it is conceivable that mutations in this pathway that result in constitutive p-Akt activity make these cell lines more susceptible to infection with certain viruses. Taken together, these data suggest that endogenous p-Akt can serve as a potential biomarker to predict sensitivity to CF33 treatment. The *in vitro* data support this concept and predicted the cell lines most sensitive to CF33 treatment, with relative resistance of the wild-type PI3K/Akt line MDA-MB-231 overcome by increasing the MOI delivered *in vitro*. This suggests that the Akt-mediated mode of entry is not the only way CF33 infects cells. This hypothesis was also supported by the *in vivo* data, as CF33 was effective in varying degrees in both MDA-MB-468 and MDA-MB-231 xenograft models based on the p-Akt status. Whereas CF33 was capable of actually reducing tumor size in the MDA-MB-468 xenografts, the virus was only able to inhibit tumor growth in the MDA-MB-231 model, even at higher intratumoral dose. Previous work on another oncolytic vaccinia virus GLV-1h68 also showed MDA-MB-231 xenografts to be difficult to treat, with poor or non-response even with high doses delivered.[27]

In summary, CF33 is a novel chimeric orthopoxvirus that shows promise as an oncolytic agent against TNBC in our initial study of

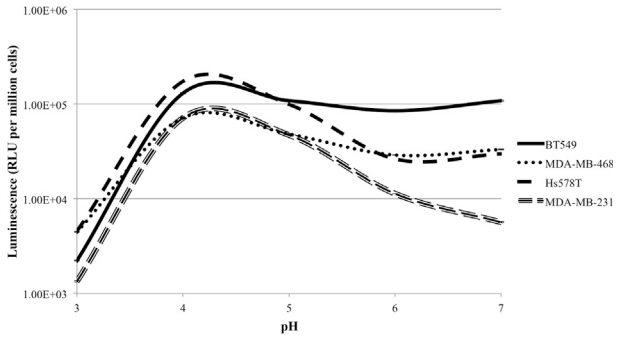

Figure 4. Viral Entry of 33-(SE)Fluc2 Is Markedly Higher in Triple-Negative Breast Cancer Cell Lines with Endogenous p-Akt Activity (BT549, Hs578T, and MDA-MB-468) Than in the Line without p-Akt Activity (MDA-MB-231) at Neutral pH

In accordance with previously reported literature of vaccinia virus, viral entry was stimulated by low pH conditions (peak entry pH 4 or 5).

its mechanism and effectiveness. It is cytotoxic against several different TNBCs, with the endogenous p-Akt level of the cell lines predicting sensitivity to CF33 infection. CF33 was also effective in two different TNBC xenograft models when administered intratumorally, demonstrating a natural tropism for tumor cells without significant systemic toxicity at the dosages tested. Further experiments to elucidate its effectiveness against other cancer types, its mechanism of action, and genetic modification to enhance its specificity against tumor cells are needed.

MATERIALS AND METHODS

Cell Culture and Cell Lines

Human TNBC cell lines MDA-MB-231 (kindly provided by Dr. Sangkil Nam, City of Hope), MDA-MB-468 (kindly provided by Dr. John Yim, City of Hope), BT549 (Dr. Yim), and Hs578T (Dr. Yim) were cultured in RPMI 1640 (Corning, Corning, NY) supplemented with 10% fetal bovine serum (FBS) and 1% antibiotic-antimycotic solution. All TNBC lines were tested and verified as authentic by Genetica Cell Line Testing (Burlington, NC). African green monkey kidney fibroblasts (CV-1) were obtained from American Type Culture Collection (ATCC) (Manassas, VA) and cultured in DMEM (Corning, Corning, NY) supplemented with 10% FBS and 1% antibiotic-antimycotic solution. All media and supplements were purchased from Corning (Corning, NY). All cells were grown at 37°C in a 5% CO_2-humidified incubator.

Viruses

Cowpox virus strain Brighton; raccoonpox virus strain Herman; rabbitpox virus strain Utrecht; and VACV strains WR, IHD, Elstree, CL, Lederle-Chorioallantoic, and AS were purchased from ATCC. All orthopoxvirus strains were grown and titrated in CV-1 cells.

Development and Selection of Chimeric Orthopoxvirus

To generate a pool of chimeric orthopoxviruses, CV-1 cells were co-infected with cowpox virus strain Brighton; raccoonpox virus strain Herman; rabbitpox virus strain Utrecht; and VACV strains WR, IHD, Elstree, CL, Lederle-Chorioallantoic, and AS. Cells were harvested three days after infection. One hundred chimeric orthopoxvirus plaques were picked from CV-1 cells infected with the chimeric orthopoxvirus pool. These 100 plaques were further plaque purified two more times in CV-1 cells to yield 100 clonally purified individual chimeric virus isolates, which, together with the parental viruses, were subjected to high-throughput screening against the NCI-60 cell lines. Isolate CF33 demonstrated the most potent tumoricidal properties against the NCI-60 cell lines and was chosen for this study given that it performed comparably or better than its parental strains against the TNBC lines in the NCI-60 panel at low screening MOI (Figure S2).

Generation of Luciferase-Expressing CF33 (33-(SE)FLuc2)

To construct thymidine kinase (TK) shuttle vector, the left and right flanking sequences of the *TK* gene of CF33 chimeric orthopoxvirus were PCR amplified from CF33 genomic DNA using Q5 High-Fidelity 2X Master Mix (New England Biolabs, Ipswich, MA) and the following primers: 5′- GCGCATATGATCTATGGATTACCATG GATGACAACTC-3′ and 5′- CGTTTAACTCGTCTAATTAATTC TGTAC-3′ (left flank) and 5′- CAGGTAAAAGTACAGAATTAAT TAGACGAGTTAAACGAGC TCGTCGACGGATCCGCTAGCG GCCGCGGAGGTAATGATATGTATCAATCGGTGTGTAG-3′ and 5′- GCGGAATTCGTAATTACTTAGTAAATCCGCCGTAC TAGG-3′ (right flank). The two fragments were joined together using the method of gene splicing by overlapping extension.[5] The resulting fragment was digested with *Nde* I and *Eco*R I and cloned into the same-cut plasmid pGPT to yield p33NC-TK. The flanking sequences of *TK* in the shuttle vector were confirmed by sequencing. p33NC-TK contains the left and right flanking sequences of *TK* separated by *Sac*I, SalI, *BamH*I, *Nhe*I, and *Not*I and *Escherichia coli* guanine phosphoribosyltransferase (gpt) gene driven by the vaccinia virus (VACV) early promoter p7.5E as a transient dominant selectable marker.

The hNIS expression cassette with the VACV SE was PCR-amplified using Q5 High-Fidelity 2X Master Mix (New England Biolabs, Ipswich, MA) and the following primers: 5′- GCGAAGCTTGAGCT CAAAAATTGAAAAACTAGCGTCTTTTTTTGCTCGAAGTCGA CCACCATGGAGGCCGTGGAG-3′ and 5′- GCGGATCCATAAA AATTAATTAATCAGAGGTTTGTCTCCTGCTGGTCTCG-3′. The PCR fragment was digested with SacI and BamHI and cloned into the same-cut plasmid p33NC-TK to yield p33NCTK-SE-hNIS. To generate a shuttle vector containing the firefly luciferase expression cassette with the VACV SE promoter, the firefly luciferase cDNA was PCR amplified from the plasmid pCDNA3.1(+)/Luc2 = tdT (a gift from Christopher Contag, Addgene plasmid #32904) using Q5 High-Fidelity 2X Master Mix (New England Biolabs, Ipswich, MA) and the following primers: 5′- GCGGTCGACCACCATGGAA GATGCCAAAAACATTAAGAA GGGCCCAGC-3′ and 5′-GCGG GATCCATAAAAATTAATTAATCACACGGCGAT CTTGCCGC CCTTCTTGGCCTTAATGAG-3′. The PCR fragment was digested with SalI and *Bam*H I and cloned into the same-cut p33NCTK-SE-hNIS replacing hNIS to yield p33NCTK-SE-Fluc2. The firefly

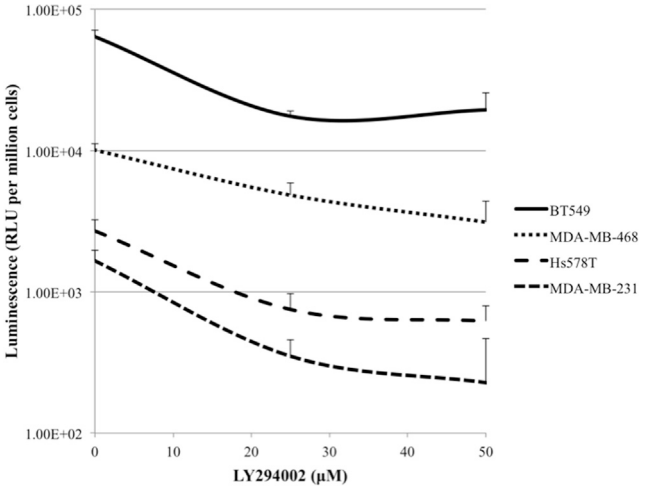

Cell line	% luminescence reduction at 50 μM LY294002
MDA-MB-231	86%
Hs578T	77%
BT549	69%
MDA-MB-231	69%

Figure 5. 33-(SE)Fluc2 Is Most Effectively Blocked by Akt Inhibitor LY294002 in the Akt/PTEN Wild-Type Cell Line MDA-MB-231 (86% Luminescence Reduction at 50 μM LY294002)

Cell lines with Akt/PTEN mutations demonstrated reduced sensitivity to LY294002 (Hs578T, 77% luminescence reduction; BT549, 69% luminescence reduction; MDA-MB-468, 69% luminescence reduction). Data are presented as means ± SD of the means.

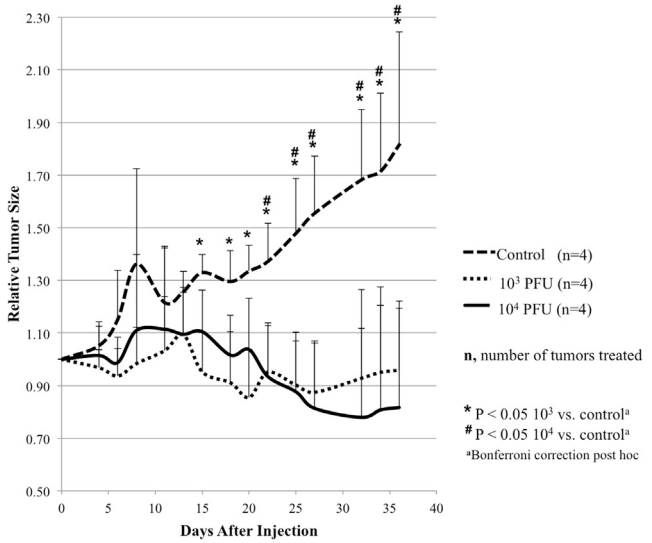

Figure 6. Intratumoral Injection of CF33 in MDA-MB-468 Xenografts Effectively Reduces Relative Tumor Size Compared to Control

Tumors were injected with PBS (control), 10^3 PFU per tumor, or 10^4 PFU per tumor. Tumor size was measured approximately every three days, and treatment effect was sustained five weeks post-injection. No significant systemic toxicity was noted as measured by body weight post-treatment. Data are presented as means ± SD of the means.

luciferase cDNA in p33NCTK-SE-Fluc2 was confirmed by sequencing. CV-1 cells were infected with CF33 at an MOI of 0.1 for 1 hr and then transfected with p33NCTK-SE-Fluc2 by use of jetPRIME *in vitro* DNA and siRNA transfection reagent (Polyplus-transfection, New York, NY). Two days post-infection, infected/transfected cells were harvested and the recombinant viruses were selected and plaque purified as described previously.[6]

Cytotoxicity Assays

Cells were seeded at 1,000 cells/well for MDA-MB-231, BT549, and Hs578T and at 3,000 cells/well for MDA-MB-468 in 96-well plates and incubated overnight. Cells were infected with 0.1, 1, and 10 MOI of each virus for MDA-MB-231 and with 0.01, 0.1, and 1 MOI for MDA-MB-468, BT549, and Hs578T. Cell viability was measured in triplicate every 24 hr for one to six days using CellTiter 96 Aqueous One solution (Promega, Madison, WI) on a spectrophotometer (Tecan Spark 10M, Mannedorf, Switzerland) at 490 nm.

Viral Replication Assays

Viral replication in TNBC was quantified using standard plaque assay. Cells were plated to confluence in 6-well plates in 2 mL growth media and then infected with 0.01 MOI of each virus. Cells were harvested in triplicate for three consecutive days. CV-1 cells were infected with serial dilutions of samples treated with CF33 in 24-well plates.

Western Blotting

TNBC cell lines were maintained in serum-free media overnight (control) or treated with CF33 over 24 hr with cell harvests at 1-, 4-, 8-, and 24-hr intervals. Whole-cell extracts were fractionated by SDS-PAGE and transferred to membrane using specified manufacturer's instruction for the apparatus (Bio-Rad, Hercules, CA). Membrane was incubated in 5% nonfat milk for 2 hr and then incubated with antibodies against p-Akt (Ser473), total-Akt, phospho-ERK (p-ERK; Thr 202/Tyr 204), total-ERK, and gapdh (all 1:1,000) overnight at 4°C (antibodies from Cell Signaling Technologies). After washing, membranes were developed with chemiluminescent reagents according to manufacturer's protocol (Bio-Rad).

Viral Entry Assays

Cells were plated at 5×10^4 cells in 24-well plates, and 33-(SE)Fluc2 at MOI 1 was adsorbed to cells for 1 hr at 4°C. Unattached virus was removed by rinsing and then cells were treated with buffers at pH 3, 4, 5, 6, and 7 for 3 min at 37°C. After rinsing, cells were incubated in growth media for 1 hr at 37°C and then harvested after adding 150 μL cell lysis reagent (Promega) for 30 min at room temperature. Then, 20 μL of this lysate was mixed with 100 μL luciferase assay substrate (Promega) and read on a spectrophotometer (Tecan) in a 96-well plate. 33-(SE)Fluc2 entry was also measured in the presence of an Akt inhibitor, LY294002 (Sigma-Aldrich, St. Louis, MO) following a similar protocol. Following treatment with buffer either

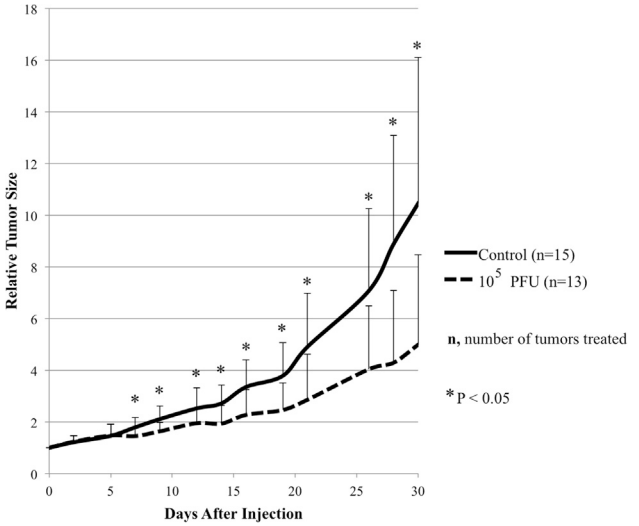

Figure 7. Intratumoral Injection of CF33 in MDA-MB-231 Xenografts Effectively Reduces Relative Tumor Size Compared to Control

Tumors were injected with PBS (control) or 10^5 PFU per tumor. Tumor size was measured approximately every three days, and treatment effect was sustained one month post-injection. Data are presented as means ± SD of the means.

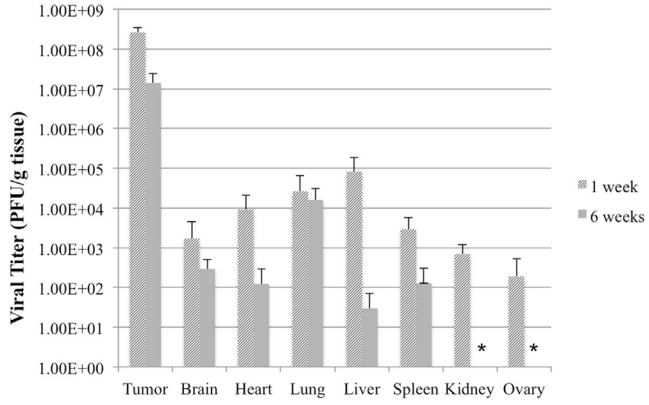

Figure 8. Viral Biodistribution of CF33 in Various MDA-MB-468 Xenograft Organs at One and Six Weeks Post-treatment

Unmodified CF33 (10^4 PFU per tumor dose) demonstrates natural tropism for tumor tissue compared to normal tissues with viral titer at least three logs higher in harvested tumor than normal tissue viral titers. Organs from three mice harvested at each time point are shown. * Indicates virus not detected. Limits of detection for kidney and ovary are 1.9×10^2 PFU/g tissue and 5.4×10^3 PFU/g tissue, respectively. Data are presented as means ± SD of the means.

pH 4 or pH 7 for 3 min at 37°C, cells were washed and incubated with growth media containing 0 μM, 25 μM, or 50 μM of LY294002 for 1 hr at 37°C. Luciferase assay was then completed as outlined above.

Orthotopic Xenograft Models

All animal studies were conducted under a City of Hope Institutional Animal Care and Use Committee (IACUC)-approved protocol (IACUC no. 15003). Fifteen Hsd:athymic Nude-*Foxn1*^{nu} female nude mice (Envigo, Indianapolis, IN) were injected with 10^7 MDA-MB-468 cells with 6 mg/mL Matrigel (Corning) in the second and fourth mammary fat pads at 12 weeks of age. When the tumors reached approximately 100–150 mm^3 in size, mice were assigned non-randomly to groups and tumors were injected intratumorally with either PBS alone (n = 4), 10^3 PFU (n = 6), or 10^4 PFU (n = 5) in 50 μL PBS. Sample size was selected based on expected effect size. Animals were assigned to treatment groups based on the average of their pre-treatment tumor sizes such that variance of tumor size did not differ significantly between the groups prior to viral injection. Tumor size was then measured every three days for six weeks. Tumor volume was calculated according to $V(mm^3) = (4/3) \times (\pi) \times (a/2)2 \times (b/2)$, where a is the smallest diameter and b is the largest diameter. No blinding was performed. Seven days following intratumoral injection, two to three mice per group were sacrificed such that tumor and organs (lung, heart, liver, kidney, spleen, ovary, and brain) were snap frozen in liquid nitrogen and used for further histopathological staining, immunohistochemical staining, and viral plaque assays. A separate xenograft model was also generated in another eight athymic nude mice by injecting 5×10^6 MDA-MB-231 cells into five locations (bilateral fourth mammary fat pads, bilateral flank, and upper back). Each tumor was injected with either PBS (n = 4) or 10^5 PFU (n = 4) when the average size of tumor was approximately 105 mm^3 in both groups without significant variance between groups. Tumor volume was calculated in the same manner as the MDA-MB-468 model.

Imaging and Staining

H&E staining of tissue sections was performed per routine protocols by our institutional pathology department. Tissue slides were stained for immunofluorescence with the primary antibody against vaccinia virus (ab35219) at 1:200 dilution (Abcam, Cambridge, MA). Slides were incubated in Tris-EDTA buffer in 100°C water bath for 30 min, cooled, and then blocked with blocking solution (TSA) for 30 min. Primary antibody was incubated overnight at 4°C, serially washed in Tween, and then incubated with the immunofluorescent secondary antibody for 60 min at room temperature (Alexa Fluor 546; Thermo Fisher, Waltham, MA). Imaging was performed using Life Technologies EVOS FL Auto imaging system (Life Technologies, Carlsbad, CA).

Statistics

Data are presented as means ± SD of the means. Representative figures are presented for *in vitro* studies with at least two replicates of the same experiment performed. Two-way ANOVA was used for comparison between more than two groups with post hoc analysis, including Bonferroni correction where applicable. Unpaired, two-tailed Student's t tests were used for comparison between two groups for the *in vivo* portions of the study without replicates.

Data Availability

The data that support the findings of this study are available from the corresponding author upon reasonable request.

SUPPLEMENTAL INFORMATION

Supplemental Information includes two figures and can be found with this article online at https://doi.org/10.1016/j.omto.2018.04.001.

AUTHOR CONTRIBUTIONS

A.H.C., Y.F., and N.G.C. conceived and designed the study. A.H.C., M.P.O., J.L., and S.-I.K. designed and performed experiments for the study. N.G.C .and J.L. generated the viruses used in this project. A.H.C., M.P.O., Y.F., and N.G.C. all contributed to the drafting of the manuscript. All authors were involved in data analysis and interpretation.

CONFLICTS OF INTEREST

The authors have no disclosures.

ACKNOWLEDGMENTS

Research reported in this publication includes work performed in the High Throughput Screening Core supported by the National Cancer Institute of the NIH under award number P30CA033572. Additional support was provided in part by the Susan E. Riley Foundation. The content is solely the responsibility of the authors and does not necessarily represent the official views of the NIH.

REFERENCES

1. Wahba, H.A., and El-Hadaad, H.A. (2015). Current approaches in treatment of triple-negative breast cancer. Cancer Biol. Med. *12*, 106–116.
2. Curigliano, G., and Goldhirsch, A. (2011). The triple-negative subtype: new ideas for the poorest prognosis breast cancer. J. Natl. Cancer Inst. Monogr. *2011*, 108–110.
3. Andtbacka, R.H., Kaufman, H.L., Collichio, F., Amatruda, T., Senzer, N., Chesney, J., Delman, K.A., Spitler, L.E., Puzanov, I., Agarwala, S.S., et al. (2015). Talimogene Laherparepvec improves durable response rate in patients with advanced melanoma. J. Clin. Oncol. *33*, 2780–2788.
4. Kaufman, H.L., Kohlhapp, F.J., and Zloza, A. (2015). Oncolytic viruses: a new class of immunotherapy drugs. Nat. Rev. Drug Discov. *14*, 642–662.
5. Horton, R.M., Ho, S.N., Pullen, J.K., Hunt, H.D., Cai, Z., and Pease, L.R. (1993). Gene splicing by overlap extension. Methods Enzymol. *217*, 270–279.
6. Falkner, F.G., and Moss, B. (1990). Transient dominant selection of recombinant vaccinia viruses. J. Virol. *64*, 3108–3111.
7. Bengali, Z., Townsley, A.C., and Moss, B. (2009). Vaccinia virus strain differences in cell attachment and entry. Virology *389*, 132–140.
8. Diehl, N., and Schaal, H. (2013). Make yourself at home: viral hijacking of the PI3K/Akt signaling pathway. Viruses *5*, 3192–3212.
9. Townsley, A.C., Weisberg, A.S., Wagenaar, T.R., and Moss, B. (2006). Vaccinia virus entry into cells via a low-pH-dependent endosomal pathway. J. Virol. *80*, 8899–8908.
10. Testa, J.R., and Bellacosa, A. (2001). AKT plays a central role in tumorigenesis. Proc. Natl. Acad. Sci. USA *98*, 10983–10985.
11. Eierhoff, T., Hrincius, E.R., Rescher, U., Ludwig, S., and Ehrhardt, C. (2010). The epidermal growth factor receptor (EGFR) promotes uptake of influenza A viruses (IAV) into host cells. PLoS Pathog. *6*, e1001099.
12. Feng, S.Z., Cao, W.S., and Liao, M. (2011). The PI3K/Akt pathway is involved in early infection of some exogenous avian leukosis viruses. J. Gen. Virol. *92*, 1688–1697.
13. Liu, Z., Tian, Y., Machida, K., Lai, M.M., Luo, G., Foung, S.K., and Ou, J.H. (2012). Transient activation of the PI3K-AKT pathway by hepatitis C virus to enhance viral entry. J. Biol. Chem. *287*, 41922–41930.
14. Tiwari, V., and Shukla, D. (2010). Phosphoinositide 3 kinase signalling may affect multiple steps during herpes simplex virus type-1 entry. J. Gen. Virol. *91*, 3002–3009.
15. Izmailyan, R., Hsao, J.C., Chung, C.S., Chen, C.H., Hsu, P.W., Liao, C.L., and Chang, W. (2012). Integrin β1 mediates vaccinia virus entry through activation of PI3K/Akt signaling. J. Virol. *86*, 6677–6687.
16. Wang, G., Barrett, J.W., Stanford, M., Werden, S.J., Johnston, J.B., Gao, X., Sun, M., Cheng, J.Q., and McFadden, G. (2006). Infection of human cancer cells with myxoma virus requires Akt activation via interaction with a viral ankyrin-repeat host range factor. Proc. Natl. Acad. Sci. USA *103*, 4640–4645.
17. Nicholson, K.M., and Anderson, N.G. (2002). The protein kinase B/Akt signalling pathway in human malignancy. Cell. Signal. *14*, 381–395.
18. Yi, K.H., and Lauring, J. (2016). Recurrent AKT mutations in human cancers: functional consequences and effects on drug sensitivity. Oncotarget *7*, 4241–4251.
19. Mukohara, T. (2015). PI3K mutations in breast cancer: prognostic and therapeutic implications. Breast Cancer (Dove Med. Press) *7*, 111–123.
20. Cossu-Rocca, P., Orrù, S., Muroni, M.R., Sanges, F., Sotgiu, G., Ena, S., Pira, G., Murgia, L., Manca, A., Uras, M.G., et al. (2015). Analysis of PIK3CA mutations and activation pathways in triple negative breast cancer. PLoS ONE *10*, e0141763.
21. Saal, L.H., Gruvberger-Saal, S.K., Persson, C., Lövgren, K., Jumppanen, M., Staaf, J., Jönsson, G., Pires, M.M., Maurer, M., Holm, K., et al. (2008). Recurrent gross mutations of the PTEN tumor suppressor gene in breast cancers with deficient DSB repair. Nat. Genet. *40*, 102–107.
22. Chagpar, R.B., Links, P.H., Pastor, M.C., Furber, L.A., Hawrysh, A.D., Chamberlain, M.D., and Anderson, D.H. (2010). Direct positive regulation of PTEN by the p85 subunit of phosphatidylinositol 3-kinase. Proc. Natl. Acad. Sci. USA *107*, 5471–5476.
23. Jamieson, S., Flanagan, J.U., Kolekar, S., Buchanan, C., Kendall, J.D., Lee, W.J., Rewcastle, G.W., Denny, W.A., Singh, R., Dickson, J., et al. (2011). A drug targeting only p110α can block phosphoinositide 3-kinase signalling and tumour growth in certain cell types. Biochem. J. *438*, 53–62.
24. Weigelt, B., Warne, P.H., and Downward, J. (2011). PIK3CA mutation, but not PTEN loss of function, determines the sensitivity of breast cancer cells to mTOR inhibitory drugs. Oncogene *30*, 3222–3233.
25. Hofmann, B.T., and Jücker, M. (2012). Activation of PI3K/Akt signaling by N-terminal SH2 domain mutants of the p85α regulatory subunit of PI3K is enhanced by deletion of its C-terminal SH2 domain. Cell. Signal. *24*, 1950–1954.
26. Quayle, S.N., Lee, J.Y., Cheung, L.W., Ding, L., Wiedemeyer, R., Dewan, R.W., Huang-Hobbs, E., Zhuang, L., Wilson, R.K., Ligon, K.L., et al. (2012). Somatic mutations of PIK3R1 promote gliomagenesis. PLoS ONE *7*, e49466.
27. Worschech, A., Chen, N., Yu, Y.A., Zhang, Q., Pos, Z., Weibel, S., Raab, V., Sabatino, M., Monaco, A., Liu, H., et al. (2009). Systemic treatment of xenografts with vaccinia virus GLV-1h68 reveals the immunologic facet of oncolytic therapy. BMC Genomics *10*, 301.

OMTO, Volume *9*

Supplemental Information

Endogenous Akt Activity Promotes Virus Entry and Predicts Efficacy of Novel Chimeric Orthopoxvirus in Triple-Negative Breast Cancer

Audrey H. Choi, Michael P. O'Leary, Jianming Lu, Sang-In Kim, Yuman Fong, and Nanhai G. Chen

Supplementary Data

Supplemental Figure 1. CF33 infects MDA-MB-468 tumors *in vivo*.
Immunofluorescent detection of polyclonal antibody against vaccinia virus demonstrates viral infection of MDA-MB-468 xenograft tumor tissue harvested one week after intratumoral CF33 injection. (A) Control tumor, 4X, (B) Control tumor, 60X, (C) Tumor treated with 10^5 PFU, 4X, (C) Tumor treated with 10^5 PFU, 60X. (VV: green; DAPI counterstain: blue).

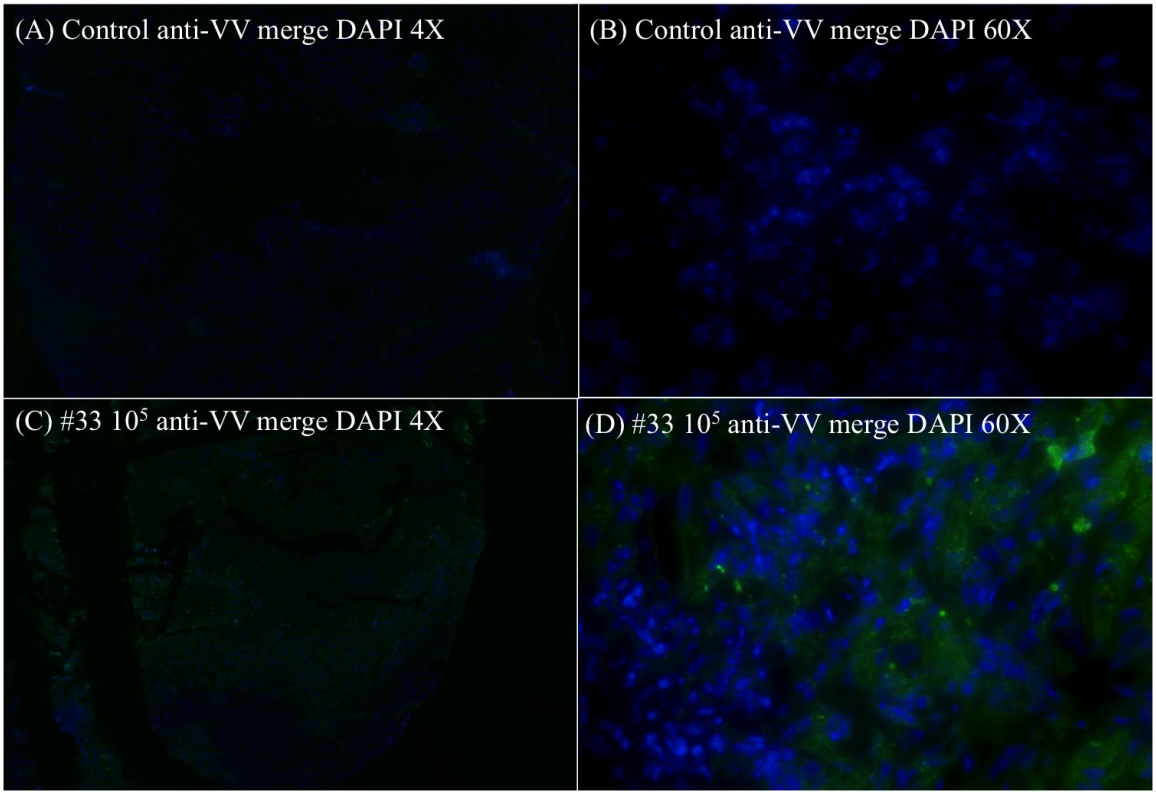

Supplemental Figure 2. High-throughput screening of CF33 against parental viruses. All cells were infected at 0.01 MOI and assayed for cell viability at 96 hours post-infection. While none of the viruses were effective against MD-MBA-231 or MD-MBA-468 at this particular screening MOI, CF33 was more effective than any of the parental viruses against BT549 and Hs578T and was thus selected for further study. Data are presented as means ± standard deviation of the means.

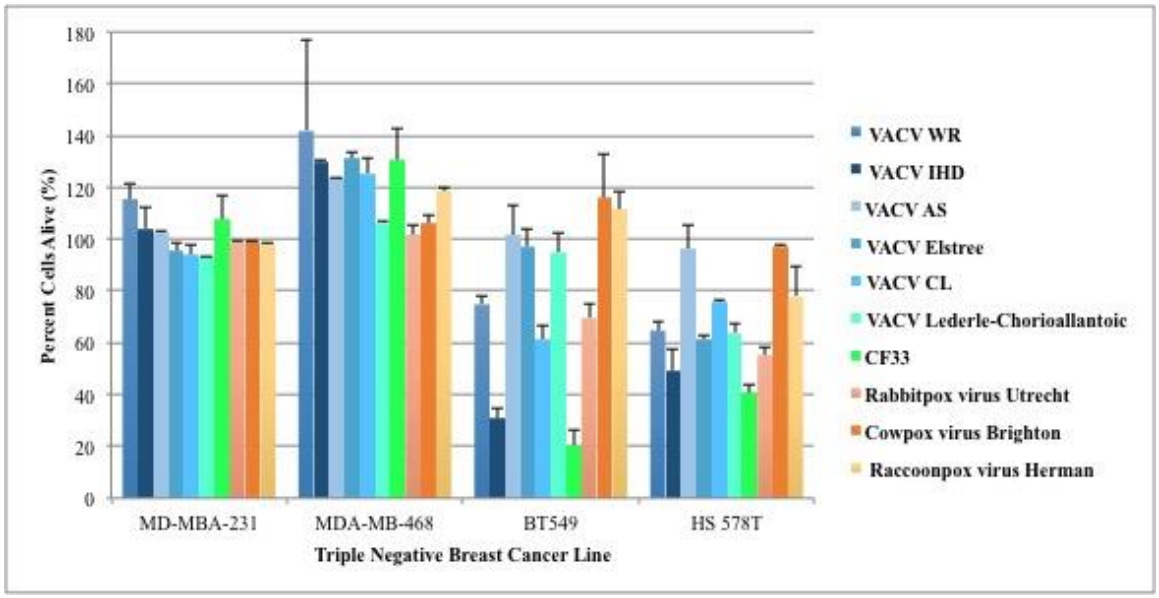

Virus	MD-MBA-231		MDA-MB-468		BT549		HS 578T	
	% Cells Alive	SD	% Cells Alive	SD	% Cells Alive	SD	% Cells Alive	SD
VACV WR	115.46	5.89	141.72	35.53	74.84	3.14	64.75	3.56
VACV IHD	104.11	8.32	129.44	1.04	30.91	3.69	49.18	8.27
VACV AS	102.31	0.92	123.57	0.52	101.56	11.86	95.97	9.80
VACV Elstree	95.36	2.89	131.09	2.33	97.22	6.36	61.42	1.65
VACV CL	94.14	3.70	125.40	5.71	61.40	5.50	75.73	0.76
VACV Lederle-Chorioallantoic	93.32	0.00	106.51	0.26	95.00	7.62	63.94	3.69
CF33	107.46	9.36	130.35	12.19	20.52	5.81	40.72	3.44
Rabbitpox virus Utrecht	99.04	0.69	101.74	3.37	69.56	5.11	55.21	3.05
Cowpox virus Brighton	99.04	0.46	105.96	3.11	116.11	17.04	97.32	0.25
Raccoonpox virus Herman	98.14	0.35	118.62	1.30	111.61	6.75	77.80	11.84